ORIGINAL RESEARCH

Simultaneous Non-Invasive Epicardial and Endocardial Mapping in Patients With Brugada Syndrome: New Insights Into Arrhythmia Mechanisms

Boris Rudic, MD;* Maria Chaykovskaya, MD;* Alexey Tsyganov, MD; Vitaly Kalinin, MD, PhD; Erol Tülümen, MD; Theano Papavassiliu, MD; Christina Dösch, MD; Volker Liebe, MD; Jürgen Kuschyk, MD; Susanne Röger, MD; Ibrahim El-Battrawy, MD; Ibrahim Akin, MD; Marina Yakovleva, MD, PhD; Elena Zaklyazminskaya, MD, PhD; Anna Shestak, MS; Stanislav Kim, MD; Mikhail Chmelevsky, MD; Martin Borggrefe, MD, PhD

***Background*—**The underlying mechanisms of Brugada syndrome (BrS) are not completely understood. Recent studies provided evidence that the electrophysiological substrate, leading to electrocardiogram abnormalities and/or ventricular arrhythmias, is located in the right ventricular outflow tract (RVOT). The purpose of this study was to examine abnormalities of epicardial and endocardial local unipolar electrograms by simultaneous noninvasive mapping in patients with BrS.

***Methods and Results*—**Local epicardial and endocardial unipolar electrograms were analyzed using a novel *n*oninvasive *e*pi- and *e*ndocardial *e*lectrophysiology *s*ystem (NEEES) in 12 patients with BrS and 6 with right bundle branch block for comparison. Fifteen normal subjects composed the control group. Observed depolarization abnormalities included fragmented electrograms in the anatomical area of RVOT endocardially and epicardially, significantly prolonged activation time in the RVOT endocardium (65±20 vs 38±13 ms in controls; P=0.008), prolongation of the activation-recovery interval in the RVOT epicardium (281±34 vs 247±26 ms in controls; P=0.002). Repolarization abnormalities included a larger area of ST-segment elevation >2 mV and T-wave inversions. Negative voltage gradient (−2.5 to −6.0 mV) between epicardium and endocardium of the RVOT was observed in 8 of 12 BrS patients, not present in patients with right bundle branch block or in controls.

***Conclusions*—**Abnormalities of epicardial and endocardial electrograms associated with depolarization and repolarization properties were found using NEEES exclusively in the RVOT of BrS patients. These findings support both, depolarization and repolarization abnormalities, being operative at the same time in patients with BrS. **(*J Am Heart Assoc*. 2016;5:e004095 doi: 10.1161/JAHA.116.004095)**

Key Words: ajmaline challenge • arrhythmia • Brugada syndrome • depolarization • electrocardiography • endocardium • epicardium • repolarization • right bundle branch block • right ventricular outflow tract • sudden death

Brugada syndrome (BrS) is an inherited arrhythmia characterized by spontaneous or induced ST elevation in right precordial electrocardiogram (ECG) leads and a high risk of sudden cardiac death, attributed to ventricular fibrillation. This disorder is estimated to be responsible for at least 4% of all sudden deaths and for at least 20% of sudden deaths in patients with structurally normal hearts.[1] In familial cases, this syndrome transmits by autosomal-dominant mode of inheritance with variable penetrance.[2,3]

From the Department of Medicine, University Medical Center Mannheim, Mannheim, Germany (B.R., E.T., T.P., C.D., V.L., J.K., S.R., I.E.-B., I.A., M.B.); German Center for Cardiovascular Research (DZHK), Partner Site Heidelberg/Mannheim, Mannheim, Germany (B.R., E.T., T.P., C.D., V.L., J.K., S.R., I.E.-B., I.A., M.B.); Petrovsky National Research Center of Surgery, Moscow, Russia (M. Chaykovskaya, A.T., M.Y., E.Z., A.S., S.K.); EP Solutions SA, Yverdon-les-Bains, Switzerland (V.K., M. Chmelevsky); Pirogov Russian National Research Medical University, Moscow, Russia (E.Z.).

Accompanying Videos S1 through S3, Data S1, Tables S1 through S7 and Figures S1 through S5 are available at http://jaha.ahajournals.org/content/5/11/e004095.full#sec-20

*Dr Rudic and Dr Chaykovskaya contributed equally to this article.

Correspondence to: Boris Rudic, MD, Department of Medicine–Cardiology, University Medical Centre Mannheim–I, Theodor-Kutzer-Ufer 1-3, Mannheim D-68167, Germany. E-mail: boris.rudic@gmail.com

Received July 18, 2016; accepted September 8, 2016.

There are 17 genes that, when mutated, can cause the disease, but most of them represent only a minority of BrS cases.[4] The only gene accounting significant portion of BrS patients is *SCN5A* gene, which encodes the α-subunit of the Nav1.5 cardiac sodium channel. Mutations in this gene can be found approximately in 15% to 30% of BrS cases.[5]

Experimental and clinical studies have provided evidence that cellular electrophysiological changes, leading to ECG abnormalities and ventricular arrhythmias, are located at the free wall region of the right ventricle outflow tract (RVOT).[6–8] Two main hypotheses have been proposed to explain the underlying mechanism of BrS.[1] Repolarization hypothesis considers that accelerated inactivation of Na^+ channels and predominance of transient outward K^+ current produce a gradient of the action potential in different layers of the RVOT at the beginning of repolarization. This gradient might trigger ventricular arrhythmias through phase 2 reentry. The depolarization hypothesis suggests that conduction delay and dispersion of conduction velocity in the RVOT at the end of ventricular depolarization may cause ECG abnormalities and initiation of ventricular tachyarrhythmias.[9]

A number of studies including catheter-based epicardial and endocardial mapping of the RVOT in humans were performed in order to investigate electrophysiological substrate of BrS. Fractionated and low-voltage (<1 mV) bipolar electrogram (EG),[10–14] prolonged duration of bipolar EG,[6,10,12,14] ST-segment elevation of unipolar EGs,[10] and activation-recovery interval (ARI) prolongation[8] were discovered in the epicardial aspect of the RVOT. The results of endocardial mapping of the RVOT were partly contradictory. No significant abnormalities of endocardial EGs were detected in several studies.[6,10,12] At the same time fractionation, prolonged duration of bipolar EGs[14,15] and late activation were identified in the epicardial aspect of the RVOT.

Previous studies have demonstrated that epicardial[10–13] or endocardial[15] ablation of the zone of abnormal EGs resulted in normalization of the 12-lead ECG and in prevention of ventricular fibrillation (VF) recurrences. In a recently published study, a novel cardiac imaging modality, noninvasive electrocardiographic imaging, was used to characterize the morphology and activation and recovery-related properties of local unipolar EGs in BrS patients in comparison with right bundle brunch block (RBBB) patients and normal subjects.[16,17] EG abnormalities, such as ST-segment elevation and fractionation of unipolar EGs, as well as conduction delay and prolongation of ARI, were found in BrS patients in the epicardial aspect of the RVOT. The results of this study were limited by only epicardially reconstructed EGs. However, methods of noninvasive reconstruction not only for epicardial, but for endocardial EGs as well have been developed recently.[18–21]

The present study investigated the morphology of local unipolar EGs and other electrophysiological properties of the heart in patients with BrS using a novel noninvasive epi- and endocardial electrophysiology system (NEEES), which allows simultaneous recording from the epi- and endocardium.

Methods

Patient Characteristics

Two groups of patients and an age- and sex-matched control group were enrolled in this study. The group of patients with BrS included 12 patients (10 males; age, 37.0±10.7 years). The diagnosis of BrS was established according to the current consensus report.[22] Six patients (5 males; age, 42.2±11.8 years) had persistent spontaneous Brugada type 1 ECG. Another 6 patients (5 males; age, 32.2±6.0 years) showed a normal 12-lead ECG pattern under baseline conditions, which converted to type 1 ECG during ajmaline challenge (0.6–1.0 mg of ajmaline/kg body weight over 5–10 minutes). Three patients had documented VF episodes in history, and in 3 patients VF was induced during the electrophysiology (EP) study. Six of 12 patients were asymptomatic and not inducible during EP study. Transthoracic echocardiography (TTE; n=12) and magnetic resonance imaging (MRI; n=6) excluded the presence of structural heart disease in BrS patients. Demographic and genetic data of BrS patients are summarized in Table 1.

The first control group consisted of 6 patients with complete RBBB (5 males; age, 37.2±10.1 years) without structural heart disease. Clinical and demographic data of RBBB patients are summarized in Table S1.

A second control group consisted of 15 patients (12 males; age 38.5±8.4 years) with various clinical indications for noninvasive mapping without overt ECG abnormalities and structural heart disease. All control patients underwent TTE and Holter monitoring. All control patients had no ECG evidence or other clinical confirmations for channelopathies. Demographic data of these patients are presented in Table S2.

The study was performed in accord with principles of the Declaration of Helsinki. Local institutional review board/ethics committee approval was obtained before study. All patients provided written informed consent to the computed tomography (CT) or MRI scanning procedures, to noninvasive mapping, and for genetic screening and agreed to data retrieval and analysis.

Genetic Screening for Known Mutations

DNA samples were extracted from venous blood by standard methods. Original pairs of polymerase chain reaction oligoprimers encompassing all coding and adjacent intronic areas of *SCN5A*, *SCN1B*, *SCN3B*, *KCNH2*, *CACNA1C*, *CACNB1*,

Table 1. Baseline Characteristics and Genetic Data of Patients With Brugada Syndrome

N	Sex	Age, y	Br Pattern on ECG		*SCN5A* Mutation Status		VT/VF	
			Baseline	Ajmaline Test	Mutation	Mutation Type	in History	During EP Study
1	Male	56	Type 1	Not performed	c.IVS24+1G>A	Splicing	Yes	Not performed
2	Male	33	Type 1	Not performed	p.R893H	Missense	No	Yes
3	Male	41	Type 1	Not performed	p.S1787N	Missense	No	No
4	Male	25	Type 1	Not performed	p.E553	Nonsense	No	No
5	Male	53	Type 1	Not performed	p.E553	Nonsense	Yes	Not performed
6	Female	41	Type 2	Positive	c.1233del	Frameshift deletion	No	Yes
7	Male	33	Type 2	Positive	None	—	Yes	Not performed
8	Male	32	Type 2	Positive	None	—	No	No
9	Female	20	Type 2	Positive	None	—	No	No
10	Male	45	Type 1	Not performed	None	—	No	Yes
11	Male	31	Type 2	Positive	None	—	No	No
12	Male	36	Type 2	Positive	None	—	No	No

Br indicates Brugada; ECG, electrocardiogram; EP, electrophysiology; VF, ventricular fibrillation; VT, ventricular tachycardia.

GPD1L, *HCN4*, and *RANGRF* genes were designed. Mutation screening in those genes was performed by bidirectional Sanger sequencing (ABI 3500; Life Technology, Carlsbad, CA) in all selected BrS patients.

Recording of Body Surface Potentials and Noninvasive Electroanatomic Mapping

The NEEES system (EP Solutions SA, Yverdon-les-Bains, Switzerland) was used for simultaneous epicardial and endocardial mapping of the heart. Up to 224 special MRI or CT scanning-compatible unipolar electrodes were placed onto the patient's torso followed by ECG-gated contrast MRI (Magnetom Avanto; Siemens Healthcare GmbH, Erlangen, Germany) or CT scanning (Somatom Definition Flash; Siemens) of the heart and torso. CT/MRI data were imported in DICOM format and semiautomatically processed by NEEES to reconstruct realistic three-dimensional (3D) models of the torso and heart. Body surface electrodes were connected to the NEEES, and ECG recordings of 5 minutes in duration during sinus rhythm were performed in all patients and controls. In 6 patients with BrS, recordings were performed at baseline and during ajmaline challenge. All ECGs were recorded with 0.05- to 500-Hz bandwidth and were digitized with the sampling rate of 1000 samples/s. Body surface ECG data were processed by NEEES, using its inverse problem solution software in combination with heart and torso anatomy, allowing for reconstruction of unipolar EGs at approximately 2500 points on epicardium and endocardium.[23,24] A brief description of the mathematical method for epicardial and endocardial computations is enclosed in Data S1 and Figure S1.

The following properties of EGs were evaluated: mean QRS voltage; mean ST segment elevation; EG fractionation; activation time (AT); activation-recovery intervals (ARIs); and epicardial and endocardial (Epi-Endo) voltage gradients (VGs). Fractionation of EG was defined as the presence of $\geq$2 intrinsic deflections with a dU/dt $\geq$0.04 V/s, separated by $\geq$10 ms. AT was defined as the interval between the beginning of the surface QRS complex and minimum derivative of the QRS in a unipolar EG. ARI was defined as the interval between times of minimum derivative of the QRS and maximum derivative of the T wave in unipolar EGs.[14] Epi-Endo VG was defined as the difference between the cardiac electrical potential (ie, unipolar EGs), reconstructed at the given point of the epicardium, and the electrical potential, reconstructed at the nearest point of the endocardium.

Noninvasive reconstruction of epicardial EGs was validated extensively in the previous studies.[25,26] For the purpose of validation of noninvasive reconstruction EGs, NEEES was used in concert with an invasive endocardial mapping in patients from the control group. Morphology of the reconstructed EGs in the RV endocardium was in agreement with the morphology of the invasively recorded EGs. An example of EG validation is presented in Figure S2.

The RVOT was depicted at the 3D heart model images in the right anterior oblique view as the area below the pulmonary valve and above the anterior border of the tricuspid valve.

Statistical Analysis

Differences among groups in categorical variables (sex, mutation status, ECG pattern, VF occurrence, response to ajmaline

challenge, and inducibility in the EP study) were examined using chi-square statistics and Fisher's exact test, as appropriate. Continuous variables were reported as means±SE and compared using the Mann–Whitney *U* test and Kruskal–Wallis test. Continuous variables at baseline and after ajmaline challenge were compared by sign test and Wilcoxon matched-pairs test. All tests with $P<0.05$ were considered statistically significant. Statistical analysis was performed using STATISTICA 10 for Windows (StatSoft, Inc, Tulsa, OK).

Results

Characteristics of EGs in Control Subjects

Characteristic patterns of local unipolar EGs in control subjects were reconstructed and analyzed (Figure 1). Clinical characteristics of patients with RBBB and control subjects are shown in Tables S1 and S2. In control subjects, high-amplitude unfractionated EGs without significant elevation or depression of ST segment were observed in most of the areas of the epicardial and endocardial surface of the ventricles. Properties of EGs in the RVOT are presented in Table 2; properties of the EGs from other areas of the ventricles are presented in Table S3.

Characteristics of Recorded EGs in BrS Patients

Significant differences in EG morphology and electrophysiological properties of local unipolar EGs between BrS patients and control subjects were found exclusively in the RVOT and, in 2 cases, in a small area of the anterior and lateral wall of the right ventricle adjacent to the RVOT. In other regions of the ventricles, unipolar EGs were similar to those in control subjects.

Typical patterns of local unipolar EGs in patients with a diagnostic type 1 ECG upon baseline are presented in Figure 2, Figure S3, and summarized in the Table S4. Properties of EGs localized in the RVOT are presented in Table 2.

Abnormal EGs on the epicardial site of the RVOT revealed ST-segment elevation >2 mV, inverted T-waves, as well as fractionation of the QRS complex. Endocardial EG abnormalities in the RVOT were represented by ST-segment elevation >2 mV. J-point elevation with ST-segment elevation and inverted T waves in EGs of the RVOT resembled classical "coved-type" BrS ECG recorded in precordial leads (Figure 2).

Quantitative parameters of the RVOT EGs in comparison to controls can be summarized as follows: (1) Mean ST elevation amounted to 6.3±5.6 versus 0.9±0.4 mV ($P<0.001$) in the epicardium and 5.8±4.0 versus 1.4±0.7 mV ($P=0.005$) in the endocardium of the RVOT in BrS patients and controls, respectively; (2) mean area in the RVOT, where elevated ST >2 mV segment was observed, amounted to 32.0±25.8 versus 0.0±0.0 cm^2 ($P<0.004$) in the epicardium and 19.8±15.6 versus 0.0±0.0 cm^2 ($P<0.001$) in the endocardium in BrS patients and controls, respectively; (3) average area of fractionated EGs amounted to 19.3±7.2 versus 0.0±0.0 cm^2 ($P<0.001$) in the epicardium and 8.6±11.7 versus 0.0±0.0 cm^2 ($P=0.004$) in the endocardium of BrS patients and controls, respectively; and (4) all patients showed increased AT in the endocardium of the RVOT and prolonged ARIs in the epicardium of the RVOT, significantly different from those for the control group in the epicardium only: 65±20 versus 38±13 ms ($P=0.008$) and 281±34 versus 247±26 ms; $P=0.022$, respectively.

Abnormal VG between the Epi-Endo VG inside the RVOT was observed in 4 of 6 patients with type 1 ECG. In these patients, a negative Epi-Endo VG (from −2.5 to −6.0 mV) appeared on the anterior and lateral part of the RVOT. In comparison, all control subjects had weak (−0.3 to −0.7 mV) uniform negative Epi-Endo VG at the entire surface of the right ventricle (RV) during the same period of measurement (Figure 3; Videos S1 and S2).

Properties of EGs in the RVOT of BrS patients with type 2 ECG are summarized in Table 2. Morphological abnormalities of the RVOT EGs in this group were represented by QRS fractionation and coved or saddleback-shaped ST elevation >2 mV; T waves of epicardial EGs were negative or biphasic.

EGs with ST elevation >2 mV in the epicardium and endocardium of the RVOT were found in 5 of 6 patients. Despite the fact that, for the above patients, ST elevation was less pronounced than in those with spontaneous type 1 ECG, the area of ST-segment elevation >2 mV significantly differed from control subjects: 13.3±8.6 versus 0.0±0.0 cm^2 ($P=0.004$) in the epicardium and 20.6±16.9 versus 0.0±0.0 cm^2 ($P<0.001$) in the endocardium.

Fractionated EGs were observed in the RVOT epicardium in all cases, but only in 1 patient in the endocardium of the RVOT. Mean area of fractionated EGs significantly differed from control subjects only in the RVOT epicardium: 11.9±4.8 versus 0±0.0 cm^2 ($P<0.004$).

Patients with type 2 BrS-ECG showed prolonged activation time in the RVOT epicardium, as compared to controls: 60±9 versus 38±13 ms ($P=0.002$). ARIs did not differ from controls. An abnormal Epi-Endo VG in the RVOT was found only in 1 of 6 patients.

Tables S5 and S6 show a detailed comparison of electrograms from the RV and left ventricle (LV) obtained in patients with a type 1 ECG and corresponding controls.

Influence of Ajmaline Challenge on Cardiac Depolarization and Repolarization Properties

Typical morphological changes of EGs induced after administration of intravenous ajmaline in all patients with

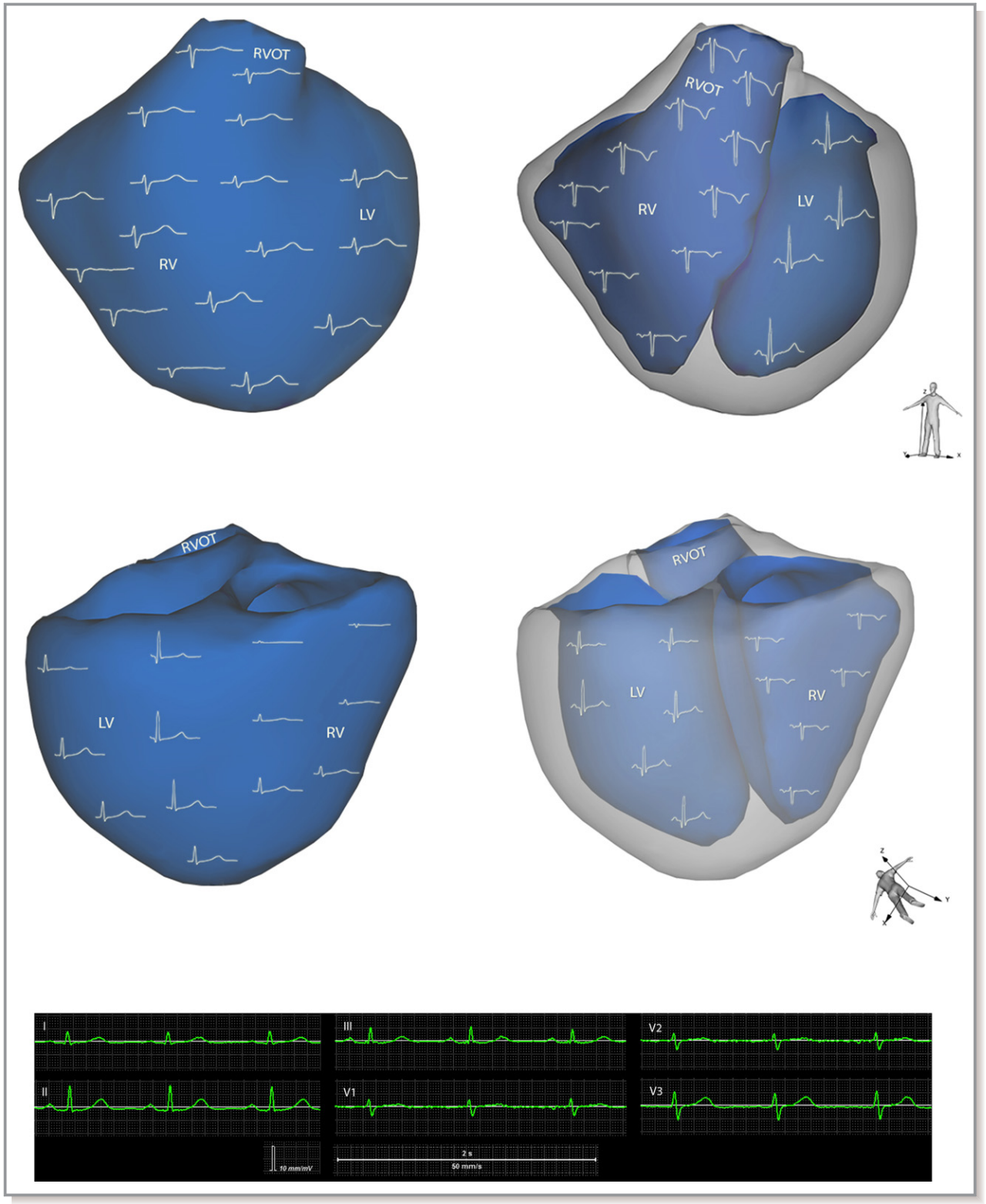

Figure 1. Recordings of local unipolar electrograms are presented (anterior and posterior view). Epicardial model on the left and endocardial model on the right, where calculations were derived from different sites of the left and right ventricle. LV indicates left ventricle; RV, right ventricle; RVOT, right ventricular outflow tract.

nondiagnostic type 1 ECG are presented in Figure S4. Detailed properties for ajmaline-provoked EGs in the RVOT are presented in Table 2. In all cases of nondiagnostic type 2 ECG, ajmaline challenge has led to a transformation of ECG and local RVOT EGs into a typical coved-type pattern, similar to those observed in patients with type 1 ECG under baseline conditions.

Table 2. EGs Properties in the RVOT for BrS Patients, RBBB Patients, and Control Subjects

Parameters	Cardiac Surface	BrS Patients With Spontaneous Type 1 (n=6)	BrS Patients With Nondiagnostic ECG Before Administration of Ajmaline (n=6)	BrS Patients With Nondiagnostic ECG After Administration of Ajmaline (n=6)	Patients With RBBB (n=6)	Control Subjects (n=15)
Area of EGs with elevated ST segment, cm^2	Epi	32.0±25.8*†	13.3±8.6*†‡	31.4±15.35*†	0.0±0.0	0.0±0.0
	Endo	19.8±15.6*†	20.6±16.9*†	27.6±12.1*†	0.0±0.0	0.0±0.0
Area of EGs with fragmentation, cm^2	Epi	19.3±7.2*†	11.9±4.8*†‡	19.5±8.2*†	0.0±0.0	0.0±0.0
	Endo	8.6±11.7*†	0.3±0.8	4.6±9.5*†	0.0±0.0	0.0±0.0
QRS voltage, mV	Epi	19.8±16.3	17.7±7.0	18.6±4.9	17.2±9.5	22.6±8.0
	Endo	26.4±19.6	29.6±18.1	29.2±9.0	23.8±14.6	29.3±18.3
Peak ST segment elevation, mV	Epi	6.3±5.6*†	1.3±1.7‡	4.8±3.8*†	1.0±0.6	0.9±0.4
	Endo	5.8±4.0*†	2.8±3.1	8.0±9.1*†	1.3±0.8	1.4±0.7
Activation time, ms	Epi	65±19†	60±9*†‡	78±12*†	102±14*	50±13
	Endo	65±20*†	53±7†‡	85±20*	91±19*	38±13
Activation-recovery interval, ms	Epi	281±34*†	247±50‡	323±43*†	244±28	247±26
	Endo	297±13	262±60	311±68	267±53	271±51
QRS duration, ms		117±29*†	97±14*†	136±37*†	168±29*	79±9
Interventricular delay, ms		14±9†	13±8†‡	25±9*†	38±11*	12±7
Epicardial-endocardial voltage gradient, mV		−3.2±3.2*†	−0.6±0.5†‡	−1.8±1.1*†	0.6±0.3*	−0.4±0.3

BrS indicates Brugada syndrome; ECG, electrocardiogram; EGs, electrograms; Endo, endocardial; Epi, epicardial; RBBB, right bundle branch block; RVOT, right ventricular outflow tract.
*P<0.05 when comparing variables between BrS and control subjects and between RBBB patients and control subjects.
†P<0.05 when comparing variables between BrS and RBBB patients.
‡P<0.05 when comparing variables between BrS patients before and after ajmaline administration.

Significant expansion of the area with elevated ST segment and fractionated EGs, as well as an increase of ST-segment elevation and ARI prolongation was observed in the endocardium and epicardium. AT was significantly increased, both in the epicardium (P=0.041) and endocardium (P=0.037). QRS duration and interventricular delay both increased after administration of ajmaline as compared to baseline. Abnormal Epi-Endo VG in the RVOT was observed in 4 of 6 patients versus 1 of 6 patients before ajmaline administration.

Difference in EGs Among Symptomatic and Asymptomatic BrS Patients

We compared the electrophysiological parameters of symptomatic and asymptomatic BrS patients, regardless of their baseline ECG (Table 3). We found a significantly larger area of ST-segment elevation >2 mV in the epicardium of the RVOT in symptomatic patients as compared to asymptomatic patients (42.3±14.2 vs 20.2±20.3 cm^2; P=0.054). Symptomatic patients had significantly lower amplitude of QRS in the epicardium (11.6±6.2 vs 26.8±10.7 mV; P=0.013) as well as in the endocardium (14.6±7.2 vs 31.3±10.3 mV; P=0.009). Finally, the RVOT AT in the endocardium was longer in symptomatic, as compared to asymptomatic, patients (87±21 vs 62±14 ms; P=0.029).

Comparison of EGs Between BrS Patients and RBBB Patients

The typical patterns of unipolar EGs in patients with RBBB are presented on Figure S5 and summarized in Table S7. Electrophysiological properties and morphology of recorded EGs significantly varied among BrS and RBBB patients. BrS patients, regardless of the baseline ECG, had fractionated EGs in the RVOT, that is, EGs with additional low-amplitude peaks of short duration. In contrast, RBBB patients had split EGs, that is, EGs with QRS divided into 2 waves of large amplitude and duration. EGs with this pattern were found not only in the RVOT, but also in most parts of the epicardium of the RV and LV. Unlike BrS patients, those with RBBB did not show EGs with significant ST-segment elevation, neither in the RVOT nor in other regions of the ventricles. A sharp increase of interventricular delay was observed in all RBBB patients. In contrast, BrS patients had no significant prolongation of interventricular delay. RBBB patients had no

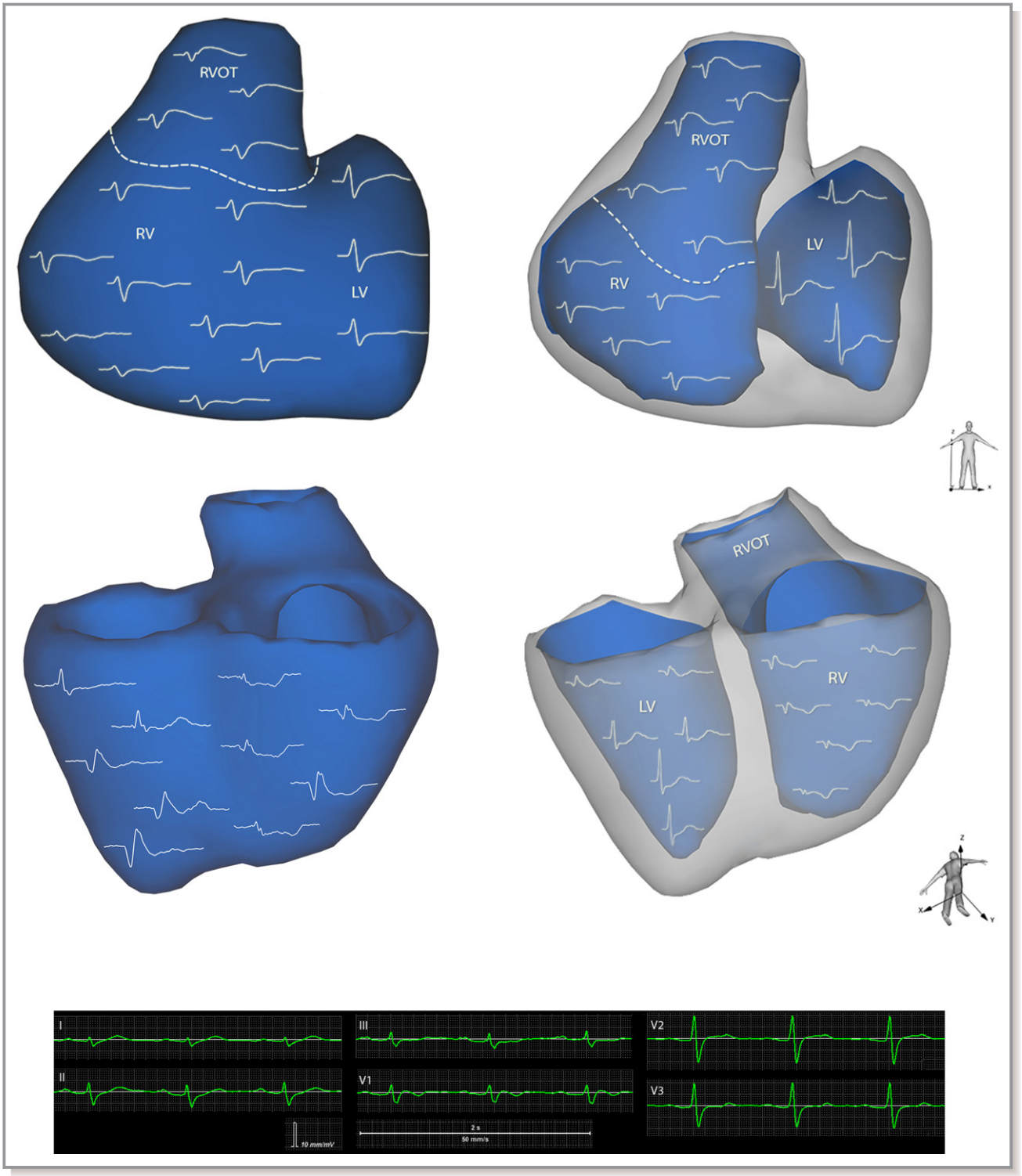

Figure 2. Recordings of local unipolar electrograms of a BrS patient with a type 1 ECG are presented. Epicardial model on the left and endocardial model on the right, where calculations were derived from different sites of the left and right ventricle (see text for detailed description). BrS indicates Brugada syndrome; ECG, electrocardiogram; LV, left ventricle; RV, right ventricle; RVOT, right ventricular outflow tract.

ARI prolongation. In all patients with RBBB during end period of QRS, the uniform weak positive Epi-Endo VG (0.02–0.8 mV) was observed in all parts of the RV, including the RVOT (Video S3).

Discussion

The relationship between epicardial and endocardial abnormalities in the RVOT of patients with BrS is still under debate.

Table 3. EGs Properties in the RVOT for BrS Patient Subgroups

Parameters	Cardiac Surface	Patients Without VF (N=6)	Patients With VF (N=6)
Area of EGs with elevated ST segment, cm^2	Epi	20.2±20.3	42.2±14.2*
	Endo	18.2±17.5	29.2±6.9
Area of EGs with fragmentation, cm^2	Epi	20.8±8.5	17.0±6.4
	Endo	6.5±12.5	6.7±9.0
QRS voltage, mV	Epi	26.8±10.7	11.6±6.2*
	Endo	31.0±10.3	14.6±7.2*
Peak ST segment elevation, mV	Epi	6.0±5.7	5.1±3.7
	Endo	5.3±6.0	8.5±7.7
Activation time, ms	Epi	87±21	62±14*
	Endo	79±13	64±17
Activation-recovery interval, ms	Epi	296±35	308±52
	Endo	284±42	314±53
QRS duration, ms		126±21	126±21
Interventricular delay, ms		14±7	14±7
Epicardial-endocardial voltage gradient, mV		−3.4±3.1	−3.4±3.1

BrS indicates Brugada syndrome; EGs, electrograms; Endo, endocardial; Epi, epicardial; RVOT, right ventricular outflow tract; VF, ventricular fibrillation.
*$P<0.05$ when comparing variables between symptomatic and asymptomatic BrS patients.

In the present study, simultaneous mapping of epicardium and endocardium was performed for the first time. Abnormal unipolar EGs in both epicardium and endocardium of the RVOT were recorded. In general, patients with BrS revealed more-pronounced electrical abnormalities on the epicardium than on the endocardium. These included depolarization abnormalities, evidenced by fractionation of EGs, delayed ventricle activation (prolonged AT), as well as repolarization abnormalities, such as coved-type ST segment, T-wave inversions, and prolonged ARIs. Abnormal electrical pattern in the endocardium consisted of coved-type ST-segment elevation, AT prolongation, and significantly less EG fractionation, as compared to EGs obtained from the epicardium. In general, the noninvasively depicted EGs changes in the RVOT were in agreement with previously described abnormalities, obtained by both invasive and noninvasive approaches.

In BrS patients with spontaneous type 1 ECG pattern ST-segment elevation and T-wave inversion can be demonstrated using a regular 12-lead ECG. For other BrS patients, it is the ajmaline challenge that can induce ECG changes similar to the above: Thus, the 12-lead ECG is not always capable of revealing BrS. At the same time, the presented noninvasive mapping technique can confirm BrS even at baseline conditions in the absence of ajmaline challenge.

Initially, BrS was described as a syndrome characterized by the atypical RBBB morphology of the ECG. The results of our study demonstrated that the similarity of ECG morphology in the right precordial leads in BrS and RBBB patients is mostly formal. The main abnormality in RBBB is increase of the interventricular delay. This phenomenon manifests as a splitting of the QRS complex into 2 waves, most predominantly at the ventricular epicardium, reflecting the sequential activation of the RV and LV. Significant ST-segment elevation,

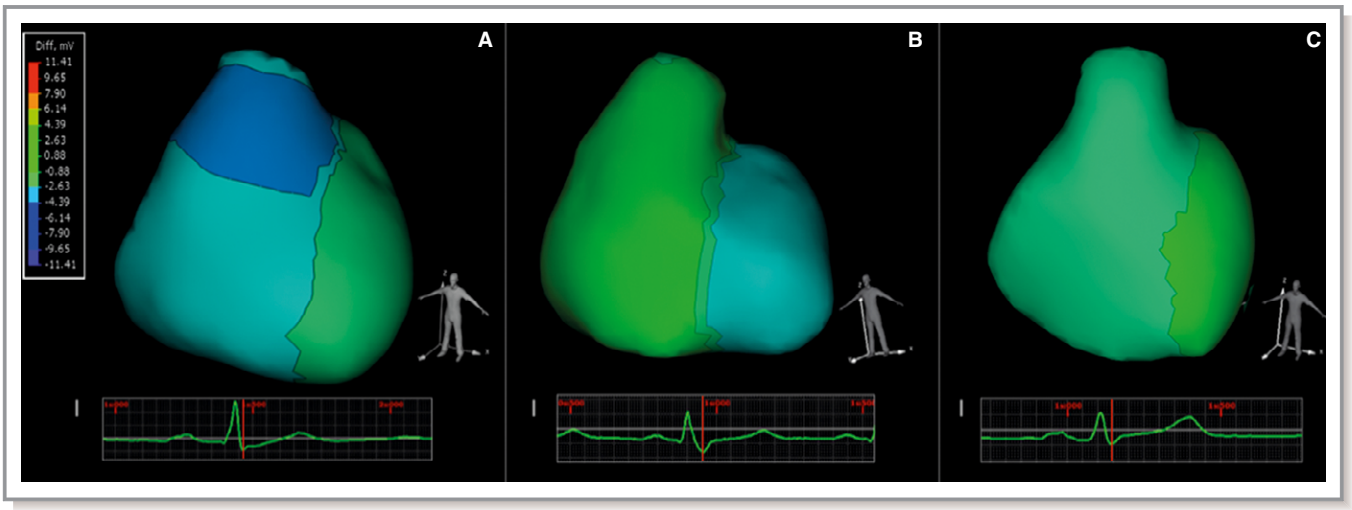

Figure 3. Epi-Endo voltage gradient at end of the ventricular depolarization in a patient with BrS and type-1 ECG (A), in a patient with RBBB (B) and in a control subject (C). Four of 6 patients with type 1 ECG, 1 of 5 patients with type 2 ECG before ajmaline administration, and 4 of 6 patient after ajmaline administration demonstrated negative Epi-Endo VG (−2.5 to −6.0 mV) in the anterior-lateral part of the RVOT (A). In contrast, during the same period, all control subjects had uniform weak negative Epi-Endo VG in the entire surface of the RV (C). All RBBB patients had uniform weak positive Epi-Edo VG in the entire surface of the RV (B). ECG, electrocardiogram; Epi-Endo, epicardial and endocardial; RBBB, right bundle branch block; RV, right ventricle; RVOT, right ventricular outflow tract; VG, voltage gradient.

fractionated EGs, and ARI prolongation are not observed in RBBB patients.

In addition, in 8 of 12 BrS patients with spontaneous or induced type 1 ECG, a significant negative VG was noted between the epicardium and endocardium of the RVOT. The underlying mechanism and the clinical value of this observation is not entirely clear. We can speculate that the Epi-Endo VG reflects asynchronous epicardial and endocardial depolarization or repolarization. It can also be associated with the deep notch of the action potential in the epicardium.

Using body surface potential mapping before and after intravenous ajmaline administration, Eckardt et al[27] observed an increase of mean body surface area of ST elevation, which correlated with the inducibility of ventricular arrhythmias during programmed ventricular stimulation in patients with BrS. This correlation was not found in a group of controls, arrhythmogenic ventricular cardiomyopathy patients, or in postmyocardial infarction patients. In the present study, we compared the EG abnormalities of symptomatic and asymptomatic BrS patients. Symptomatic patients had a significantly larger area of ST-segment elevation and lower QRS amplitudes in the RVOT using body surface potential mapping. This observation may potentially lead to a better risk stratification of asymptomatic patients with BrS. Further studies are needed to support this hypothesis.

Catheter ablation of the arrhythmogenic substrate in the RVOT identified by invasive endo- and epicardial mapping is a new, promising strategy for treatment of symptomatic BrS patients with recurrent episodes of VF. The fact that epi- and endocardial changes are present in patients with BrS may have potential clinical implications, because ablation of the arrhythmogenic substrate can be achieved by both endo-[14] and epicardial ablation.[10–12]

Conclusion

Noninvasive simultaneous mapping of the endo- and epicardium is allowing detection of the zones in the RVOT where local unipolar EGs demonstrated abnormal depolarization and repolarization in BrS patients. These abnormalities can be localized in the epicardium as well as in the endocardium and may be considered as an arrhythmogenic substrate.

Sources of Funding

The study was, in part, funded by a grant from the German Federal Ministry for Education and Research–International Bureau and by the Russian Foundation for Assistance to Small Innovative Enterprises (BMBF/IB project #01DJ4014A and FASIE award #14-1-H2.15-0001-7-P).

Disclosures

Chaykovskaya, Tsyganov and Chmelevsky are consultants to EP Solutions SA. Kalinin holds equity in EP Solutions SA. All other authors report no conflict of interest.

References

1. Antzelevitch C, Brugada P, Borggrefe M, Brugada J, Brugada R, Corrado D, Gussak I, LeMarec H, Nademanee K, Perez Riera AR, Shimizu W, Schulze-Bahr E, Tan H, Wilde A. Brugada syndrome: report of the second consensus conference. *Heart Rhythm*. 2005;2:429–440.
2. Brugada P, Brugada J. Right bundle branch block, persistent ST segment elevation and sudden cardiac death: a distinct clinical and electrocardiographic syndrome. A multicenter report. *J Am Coll Cardiol*. 1992;20:1391–1396.
3. Abriel H, Zaklyazminskaya EV. Cardiac channelopathies: genetic and molecular mechanisms. *Gene*. 2013;517:1–11.
4. Selga E, Campuzano O, Pinsach-Abuin ML, Perez-Serra A, Mademont-Soler I, Riuro H, Pico F, Coll M, Iglesias A, Pagans S, Sarquella-Brugada G, Berne P, Benito B, Brugada J, Porres JM, Lopez Zea M, Castro-Urda V, Fernandez-Lozano I, Brugada R. Comprehensive genetic characterization of a Spanish Brugada syndrome cohort. *PLoS One*. 2015;10:e0132888.
5. Chen Q, Kirsch GE, Zhang D, Brugada R, Brugada J, Brugada P, Potenza D, Moya A, Borggrefe M, Breithardt G, Ortiz-Lopez R, Wang Z, Antzelevitch C, O'Brien RE, Schulze-Bahr E, Keating MT, Towbin JA, Wang Q. Genetic basis and molecular mechanism for idiopathic ventricular fibrillation. *Nature*. 1998;392:293–296.
6. Nagase S, Kusano KF, Morita H, Fujimoto Y, Kakishita M, Nakamura K, Emori T, Matsubara H, Ohe T. Epicardial electrogram of the right ventricular outflow tract in patients with the Brugada syndrome: using the epicardial lead. *J Am Coll Cardiol*. 2002;39:1992–1995.
7. Tukkie R, Sogaard P, Vleugels J, de Groot IK, Wilde AA, Tan HL. Delay in right ventricular activation contributes to Brugada syndrome. *Circulation*. 2004;109:1272–1277.
8. Nagase S, Kusano KF, Morita H, Nishii N, Banba K, Watanabe A, Hiramatsu S, Nakamura K, Sakuragi S, Ohe T. Longer repolarization in the epicardium at the right ventricular outflow tract causes type 1 electrocardiogram in patients with Brugada syndrome. *J Am Coll Cardiol*. 2008;51:1154–1161.
9. Wilde AA, Postema PG, Di Diego JM, Viskin S, Morita H, Fish JM, Antzelevitch C. The pathophysiological mechanism underlying Brugada syndrome: depolarization versus repolarization. *J Mol Cell Cardiol*. 2010;49:543–553.
10. Nademanee K, Veerakul G, Chandanamattha P, Chaothawee L, Ariyachaipanich A, Jirasirirojanakorn K, Likittanasombat K, Bhuripanyo K, Ngarmukos T. Prevention of ventricular fibrillation episodes in Brugada syndrome by catheter ablation over the anterior right ventricular outflow tract epicardium. *Circulation*. 2011;123:1270–1279.
11. Sacher F, Jesel L, Jais P, Haissaguerre M. Insight into the mechanism of Brugada syndrome: epicardial substrate and modification during ajmaline testing. *Heart Rhythm*. 2014;11:732–734.
12. Cortez-Dias N, Placido R, Marta L, Bernardes A, Sobral S, Carpinteiro L, de Sousa J. Epicardial ablation for prevention of ventricular fibrillation in a patient with Brugada syndrome. *Rev Port Cardiol*. 2014;33:305.e301–307.
13. Brugada J, Pappone C, Berruezo A, Vicedomini G, Manguso F, Ciconte G, Giannelli L, Santinelli V. Brugada syndrome phenotype elimination by epicardial substrate ablation. *Circ Arrhythm Electrophysiol*. 2015;8:1373–1381.
14. Postema PG, van Dessel PF, de Bakker JM, Dekker LR, Linnenbank AC, Hoogendijk MG, Coronel R, Tijssen JG, Wilde AA, Tan HL. Slow and discontinuous conduction conspire in Brugada syndrome: a right ventricular mapping and stimulation study. *Circ Arrhythm Electrophysiol*. 2008;1:379–386.
15. Sunsaneewitayakul B, Yao Y, Thamaree S, Zhang S. Endocardial mapping and catheter ablation for ventricular fibrillation prevention in Brugada syndrome. *J Cardiovasc Electrophysiol*. 2012;23(suppl 1):S10–S16.
16. Zhang J, Sacher F, Hoffmayer K, O'Hara T, Strom M, Cuculich P, Silva J, Cooper D, Faddis M, Hocini M, Haissaguerre M, Scheinman M, Rudy Y. Cardiac electrophysiological substrate underlying the ECG phenotype and electrogram abnormalities in Brugada syndrome patients. *Circulation*. 2015;131:1950–1959.
17. Chaykovskaya M, Rudic B, Tsyganov A, Zaklyazminskaya E, Yakoleva MV, Borggrefe M. The use of noninvasive ECG imaging for examination of a patient with Brugada syndrome. *HeartRhythm Case Rep*. 2015;1:260–263.

18. Berger T, Fischer G, Pfeifer B, Modre R, Hanser F, Trieb T, Roithinger FX, Stuehlinger M, Pachinger O, Tilg B, Hintringer F. Single-beat noninvasive imaging of cardiac electrophysiology of ventricular pre-excitation. *J Am Coll Cardiol*. 2006;48:2045–2052.
19. van Dam PM, Oostendorp TF, Linnenbank AC, van Oosterom A. Non-invasive imaging of cardiac activation and recovery. *Ann Biomed Eng*. 2009;37:1739–1756.
20. Erem B, Coll-Font J, Orellana RM, Stovicek P, Brooks DH. Using transmural regularization and dynamic modeling for noninvasive cardiac potential imaging of endocardial pacing with imprecise thoracic geometry. *IEEE Trans Med Imaging*. 2014;33:726–738.
21. Wissner E, Revishvili A, Metzner A, Tsyganov A, Kalinin V, Lemes C, Saguner AM, Maurer T, Deiss S, Sopov O, Labarkava E, Chmelevsky M, Kuck KH. Noninvasive epicardial and endocardial mapping of premature ventricular contractions. *Europace*. 2016; May 20. pii: euw103. [Epub ahead of print]
22. Bayes de Luna A, Brugada J, Baranchuk A, Borggrefe M, Breithardt G, Goldwasser D, Lambiase P, Riera AP, Garcia-Niebla J, Pastore C, Oreto G, McKenna W, Zareba W, Brugada R, Brugada P. Current electrocardiographic criteria for diagnosis of Brugada pattern: a consensus report. *J Electrocardiol*. 2012;45:433–442.
23. Bokeriia LA, Revishvili A, Kalinin AV, Kalinin VV, Liadzhina OA, Fetisova EA. [Hardware-software system for noninvasive electrocardiographic examination of heart based on inverse problem of electrocardiography]. *Med Tekh*. 2008;1:1–7.
24. Revishvili AS, Wissner E, Lebedev DS, Lemes C, Deiss S, Metzner A, Kalinin VV, Sopov OV, Labartkava EZ, Kalinin AV, Chmelevsky M, Zubarev SV, Chaykovskaya MK, Tsiklauri MG, Kuck KH. Validation of the mapping accuracy of a novel non-invasive epicardial and endocardial electrophysiology system. *Europace*. 2015;17:1282–1288.
25. Burnes JE, Ghanem RN, Waldo AL, Rudy Y. Imaging dispersion of myocardial repolarization, I: comparison of body-surface and epicardial measures. *Circulation*. 2001;104:1299–1305.
26. Ghanem RN, Burnes JE, Waldo AL, Rudy Y. Imaging dispersion of myocardial repolarization, II: noninvasive reconstruction of epicardial measures. *Circulation*. 2001;104:1306–1312.
27. Eckardt L, Bruns HJ, Paul M, Kirchhof P, Schulze-Bahr E, Wichter T, Breithardt G, Borggrefe M, Haverkamp W. Body surface area of ST elevation and the presence of late potentials correlate to the inducibility of ventricular tachyarrhythmias in Brugada syndrome. *J Cardiovasc Electrophysiol*. 2002;13:742–749.

Supplemental Material

Data S1 - Supplemental Methods

Numerical Algorithm for Solving of Inverse Problem of Electrocardiography

1 Mathematical statement

Inverse problem of electrocardiography is a problem of numerical reconstruction of the electrical field potentials on a heart surface from the electrocardiograms registered on a surface of human body. For details refer to Figure S1.

Consider a domain Ω in $\mathbb{R}^3$ space bounded outside by a closed surface Γ_B and inside by a closed surface Γ_H, see Fig. S1. For each instant time t_k, $k = 1, 2, \ldots, T$ corresponding to body surface ECG measurements we consider the following boundary value problem. Find a function $u(x)$, $x \in \Omega$ such that

$$\Delta u = 0, \quad x \in \Omega, \tag{1}$$

$$u(x) = \varphi(x), \quad x \in \Gamma_B, \tag{2}$$

$$\frac{\partial u(x)}{\partial n} = 0, \quad x \in \Gamma_B, \tag{3}$$

where $u(x)$ is an electrical field potential, $\varphi(x)$ is the known ECG measurements on a body surface.

Equation (1) means that there are no electrical sources in the domain Ω and that the volume between heart surface Γ_H and body surface Γ_B is a passive conductor. Condition (2) is the known ECG values on body surface. In general we need ECG measurements on whole body surface. That is why we are using the body surface ECG mapping data instead of standard 12-lead ECG. Condition (3) states that there is no electrical current outside the domain and that on a body surface we have only tangential component of the electrical field flux.

Problem (1)–(3) is called Cauchy problem for the Laplace equation in mathematical theory of partial differential equations. This type of problem is ill-posed. One of the most essential properties of its ill-posedness is the instability of the potential $u(x)$ under small changes in the original data $\varphi(x)$. To solve this type of problem numerically we should first formulate the discrete statement of the problem and then apply some regularization techniques.

2 System of linear equations

For discrete statement of the problem we are using the boundary element method. The surface $\partial\Omega = \Gamma_B \cup \Gamma_H$ is approximated by the polygonal mesh S which consists of the union of N plane triangles ζ, referred to as boundary elements, $S = \zeta_1 \cup \zeta_2 \cup \ldots \cup \zeta_N$. The set of boundary elements forms a boundary element mesh. The nodes of the boundary-element mesh are defined as the points $x_i \in S$, $i = 1, 2, \ldots, N$ placed at the centers of the boundary elements ζ_i.

On the surface S we are introducing a system of linearly independent compactly supported basis functions $\phi_j(x)$, $x \in S$, $j = 1, 2, \ldots, N$, which are defined as follows:

$$\phi_j(x) = 1, \quad x \in \zeta_j,$$
$$\phi_j(x) = 0, \quad x \notin \zeta_j.$$

The functions $u(x)$ and $\frac{\partial u(x)}{\partial n}$ are approximated in the form of the expansion in the system of basis functions $\phi(x)$

$$\begin{aligned} \tilde{u}(x) &= \sum_{j=1}^{N} \alpha_j \phi_j(x), \\ \frac{\partial \tilde{u}(x)}{\partial n} &= \sum_{j=1}^{N} \beta_j \phi_j(x), \end{aligned} \tag{4}$$

where the expansion coefficients α_j and β_j are the values of the functions $u(x)$ and $\frac{\partial u(x)}{\partial n}$ at the nodes of the boundary-element mesh.

For each nodal point x_i we can write a discrete analog of the third Green formula

$$\frac{1}{2}\tilde{u}(x_i) = \int\limits_S \frac{\partial \tilde{u}(x)}{\partial n_y} \Phi(x_i, y)\, ds_y - \int\limits_S \tilde{u}(x) \frac{\partial \Phi(x_i, y)}{\partial n_y}\, ds_y,$$

where $i = 1, 2, \ldots, N$, $y \in S$,

$$\Phi(x_i, y) = \frac{1}{4\pi} \frac{1}{\|x_i - y\|}$$

is a fundamental solution of Laplace equation.

Together with (4) we are getting the system of linear equations for α_j and β_j

$$\frac{1}{2}\alpha_i + \sum_{j=1}^{N} \alpha_j \int\limits_{\zeta_j} \frac{\partial \Phi(x_i, y)}{\partial n_y}\, ds_y = \sum_{j=1}^{N} \beta_j \int\limits_{\zeta_j} \Phi(x_i, y) ds_y,$$

where $i = 1, 2, \ldots, N$, $j = 1, 2, \ldots, N$, which can be represented in the matrix form as

$$H\mathbf{u} = G\mathbf{q}, \tag{5}$$

$\mathbf{u} = [\alpha_1, \alpha_2, \ldots, \alpha_N]^T$ and $\mathbf{q} = [\beta_1, \beta_2, \ldots, \beta_N]^T$, where matrices H and G are computed as follows:

$$H \equiv [h_{ij}] = \begin{cases} \displaystyle\int\limits_{\zeta_j} \frac{\partial \Phi(x_i, y)}{\partial n_y}\, ds_y, & i \neq j, \\ \displaystyle\int\limits_{\zeta_j} \frac{\partial \Phi(x_i, y)}{\partial n_y}\, ds_y + \frac{1}{2}, & i = j, \end{cases}$$

$$G \equiv [g_{ij}] = \int\limits_{\zeta_j} \Phi(x_i, y)\, ds_y.$$

It is convenient to write (5) in a block matrix form

$$\begin{bmatrix} H_{BB} & H_{BH} \\ H_{HB} & H_{HH} \end{bmatrix} \begin{bmatrix} \mathbf{u}_B \\ \mathbf{u}_H \end{bmatrix} = \begin{bmatrix} G_{BB} & G_{BH} \\ G_{HB} & G_{HH} \end{bmatrix} \begin{bmatrix} 0 \\ \mathbf{q}_H \end{bmatrix}$$

or as a system of linear equations

$$\begin{aligned} H_{BB}\,\mathbf{u}_B + H_{BH}\,\mathbf{u}_H &= G_{BH}\,\mathbf{q}_H \\ H_{HB}\,\mathbf{u}_B + H_{HH}\,\mathbf{u}_H &= G_{HH}\,\mathbf{q}_H \end{aligned}, \tag{6}$$

where $\mathbf{u}_B$ is a numerical approximation of the potential on a Γ_B surface, $\mathbf{u}_H$ is a numerical approximation of the potential on a Γ_H surface, $\mathbf{q}_H$ is a numerical approximation of the potential normal derivative on a Γ_H surface.

Properties of the block matrices are the following:

- matrices G_{BH}, H_{BH}, H_{HB} are ill conditioned and can not be inverted without regularization;
- matrices G_{HH}, H_{BB}, H_{HH} are well conditioned and can be inverted.

3 Numerical solving of the system of linear equations

The system of linear equations (6) is solved by the following iteration procedure

$$\mathbf{q}_H^{(0)} = \mathbf{q}_0 \tag{7}$$

$$\mathbf{u}_H^{(2k)} = H_{HH}^{-1}(G_{HH}\mathbf{q}_H^{(2k-1)} - c_2) \tag{8}$$

$$\mathbf{q}_H^{(2k+1)} = G_{BH}^{-1}(H_{BH}\mathbf{u}_H^{(2k)} + c_1) \tag{9}$$

For inverting of the ill conditioned matrix G_{BH} we are using the Tikhonov regularization

$$G_{BH}^{-1} = (G_{BH}^T G_{BH} + \alpha^{(k)} R^T R)^{-1} G_{BH}^T, \tag{10}$$

where $\alpha > 0$ is a regularization parameter, R is a constrain matrix. The number of iterations is determined by the discrepancy principle.

Table S1. Demographic data of patients with bundle-branch-block.

Total number	Sex	Age	PVC	PAC	Paroxysmal lone AFib
6	Male, 5	37.2±10.1	2 (33%)	3 (50%)	1 (17%)

PVC, premature ventricular contraction; PAC, premature atrial contraction; AFib, atrial fibrillation.

Table S2. Demographic data of control subjects.

Total number	Sex	Age	PVC	PAC	AVNRT	Paroxysmal lone AFib
15	Male, 12	38.5±8.4	5 (33%)	6 (40%)	2 (13%)	2 (13%)

PVC, premature ventricular contraction; PAC, premature atrial contraction; AVNRT, atrioventricular nodal reentrant tachycardia; AFib, atrial fibrillation.

Table S3. Morphology of local unipolar EGs in control subjects.

Surface of the ventricle			Epicardium		Endocardium	
			QRS	T wave	QRS	T wave
RV	RVOT		rSr, rS, RS	Flattened or positive	rSr, rS	Negative
	Anterior	Medium	RS	Positive	rS, RS	Negative
		Apical	RS	Positive	RS	Negative or positive
	Lateral	Basal	rS	Flattened, positive	rS	Flattened
		Medium	RS	Positive	RS	Negative, positive
		Apical	Rs	Positive	RS	Negative, positive
	Posterior	Basal	Qr	Flattened, negative, positive	rS	Flattened
		Medium	QR or fractionated low amplitude	Positive	RS	Positive
		Apical	qRs	Positive	RS	Positive
	Septum	Basal	-	-	rS	Flattened
		Medium	-	-	QS or rS	Negative, positive
		Apical	-	-	QS or rS	Negative , positive
LV	Anterior	Basal	qR or fractionated low amplitude	Flattened, positive, negative	QR, qR	Flattened, positive, negative
		Medium	qRs, Rs	Positive	qR	Positive
		Apical	qRs, Rs	Positive	qR	Positive
	Lateral	Basal	qR	Flattened, positive, negative	qR	Flattened, positive
		Medium	qRs, Rs	Positive	qR	Positive
		Apical	qRs, Rs	Positive	qR, qRs	Positive
	Posterior	Basal	Qr, qR	Flattened	qR	Flattened, negative
		Medium	Qr, QR or fractionated low amplitude	Positive	qR, qRs	Positive
		Apical	qR, qRs	Positive	qRs	Positive
	Septum	Basal	-	-	Qr, QR	Negative, Flattened
		Medium	-	-	Qr, QR	Positive
		Apical	-	-	qRs	Positive

RV, right ventricle; LV, left ventricle; RVOT, right ventricular outflow tract.

Table S4. Morphology of local unipolar EGs in BrS patients with 1-type ECG.

Surface of the ventricle			Epicardium		Endocardium	
			QRS complex	T wave	QRS complex	T wave
RV	RVOT		rSr, rS, RS, fractionated; J-point elevation	Negative after coved-type elevated ST segment	rSr, rS; J-point elevation	Negative after coved-type elevated ST segment
	Anterior	Medium	RS	Positive	rS, RS	Negative
		Apical	RS	Positive	RS	Negative or positive
	Lateral	Basal	rS	Flattened, positive	rS	Flattened
		Medium	RS	Positive	RS	Negative, positive
		Apical	Rs	Positive	RS	Negative, positive
	Posterior	Basal	Qr	Flattened, negative, positive	rS	Flattened
		Medium	QR or fractionated low amplitude	Positive	RS	Positive
		Apical	qRs	Positive	RS	Positive
	Septum	Basal	-	-	rS	Flattened
		Medium	-	-	QS or rS	Negative, positive
		Apical	-	-	QS or rS	Negative, positive
LV	Anterior	Basal	qR or fractionated low amplitude	Flattened, positive, negative	QR, qR	Flattened, positive, negative
		Medium	qRs, Rs	Positive	qR	Positive
		Apical	qRs,Rs	Positive	qR	Positive
	Lateral	Basal	qR	Flattened, positive, negative	qR	Flattened, positive
		Medium	qRs,Rs	Positive	qR	Positive
		Apical	qRs,Rs	Positive	qR, qRs	Positive
	Posterior	Basal	Qr, qR	Flattened	qR	Flattened, negative
		Medium	Qr, QR or fractionated low amplitude	Positive	qR, qRs	Positive
		Apical	qR, qRs	Positive	qRs	Positive
	Septum	Basal	-	-	Qr,QR	Negative, flattened
		Medium	-	-	Qr,QR	Positive
		Apical	-	-	qRs	Positive

RV, right ventricle; LV, left ventricle; RVOT, right ventricular outflow tract.

Table S5. Comparison of electrograms obtained in the right ventricle (excluding the RVOT area) between patients with BrS type-1 ECG and control subjects.

Parameters	Cardiac surface	BrS patients with spontaneous BrS type-1				Control subjects			
		RV free wall	RV septum	RV basal posterior	RV apex	RV free wall	RV septum	RV basal posterior	RV apex
Total area of EGs with elevated ST segment, cm^2	*Epi*	0.0	-	0.0	0.0	0.0	-	0.0	0.0
	Endo	0.0	0.0	0.0	0.0	0.0	0.0	0.0	0.0
Total area of EGs with fragmentation, cm^2	*Epi*	0.0	-	4.2±3.5	0.0	0.0	-	3.8±3.4	0.0
	Endo	0.0	0.0	0.0	0.0	0.0	0.0	0.0	0.0
Mean QRS voltage, mV	*Epi*	16.7±7.4	-	12.7±6.5	26.8±10.2	18.8±8.1	-	11.7±5.3	24.1±9.3
	Endo	27.4±9.3	26.1±8.8	17.9±7.6	31.4±12.3	28.2±9.5	25.3±7.6	16.7±6.4	30.7±7.2
Mean peak ST segment elevation, mV	*Epi*	1.1±0.7	-	0.5±0.3	0.4±0.3	0.9±0.6	-	0.5±0.4	0.6±0.4
	Endo	1.4±0.9	0.7±0.5	0.6±0.4	0.8±0.7	1.1±0.7	0.7±0.04	0.6±0.5	0.7±0.4
Mean ARI, ms	*Epi*	247±25	-	236±32	228±18	232±30	-	240±35	226±25
	Endo	238±29	245±28	242±34	230±23	241±28	237±24	247±29	234±27

RV, right ventricle; RVOT, right ventricular outflow tract; EG, electrogram; ARI, activation-recovery interval.

Table S6. Comparison of electrograms obtained in the left ventricle between patients with BrS type-1 ECG and control subjects.

Parameters	Cardiac surface	BrS patients with spontaneous BrS type-1 ECG (N=6)				Control subjects (N=15)			
		LV free wall	LV septum	LV basal posterior	LV apex	LV free wall	LV septum	LV basal posterior	LV apex
Total area of EGs with elevated ST segment, cm^2	*Epi*	0.0	-	0.0	0.0	0.0	-	0.0	0.0
	Endo	0.0	0.0	0.0	0.0	0.0	0.0	0.0	0.0
Total area of EGs with fragmentation, cm^2	*Epi*	0.0	-	2.7±1.3	0.0	0.0	-	2.9±1.8	0.0
	Endo	0.0	0.0	0.0	0.0	0.0	0.0	0.0	0.0
Mean QRS voltage, mV	*Epi*	20.3±6.1	-	15.7±8.7	26.8±10.7	22.5±5.6	-	16.2±6.0	27.7±8.8
	Endo	31.4±9.0	19.8±9.4	21.0±8.8	37.2±12.3	33.8±12.4	16.6±7.5	19.9±8.7	34.0±11.5
Mean peak ST segment elevation, mV	*Epi*	0.5±0.4	-	0.3±0.3	0.2±0.3	0.6±0.4	-	0.2±0.3	0.1±0.2
	Endo	0.6±0.5	0.6±0.5	0.4±0.5	0.4±0.3	0.8±0.4	0.5±0.4	0.3±0.4	0.5±0.3
Mean ARI, ms	*Epi*	223±22	-	244±35	219±21	227±19	-	250±37	226±17
	Endo	227±24	227±28	240±42	223±27	234±23	231±27	247±29	230±20

LV, left ventricle; EG, electrogram; ARI, activation-recovery interval.

Table S7. Morphology of local unipolar EGs in patients with RBBB.

Surface of the ventricle			Epicardium		Endocardium	
			QRS complex	T wave	QRS complex	T wave
RV	RVOT		RSRS, (W-shape), RsrS	Negative	QR (with wide R)	Negative
	Anterior	Medium	RSR (M-shape)	Negative	QR (with wide R)	Negative
		Apical	RSR, rSR (M-shape), rSr, RSRs	Negative	QR (with wide R), QRsr	Negative
	Lateral	Basal	rsR, RsR (M-	Negative	QR (with	Negative

			shape)		wideR)	
		Medium	RSR (M-shape), RSRs	Negative	QR (with wideR), QRsr	Negative
		Apical	RSR (M-shape), rSR, RSRs	Negative	QR (with wideR), QRsr	Negative
	Posterior	Basal	RsRRsR (M-shape)	Negative	QR (with wideR)	Negative
		Medium	RSR (M-shape), RSRs	Negative	QR (with wideR),	Negative

					QRsr	
		Apical	RSR (M-shape), rSR’, RSRs	Negative	QR (with wide R), QRsr	Negative
	Septum	Basal	-	-	QrsR’ (W-shape)	Negative
		Medium	-	-	QrsR’ (W-shape)	Negative
		Apical	-	-	QrsR’ (W-shape)	Negative

LV	Anterior	Basal	RsrS’	Flattened	qRs, Rs (wide slurred S)	Positive
		Medium	RsrR’	Positive	qRs, Rs (wide slurred S)	Positive
		Apical	RSRS (W-shape), RSrs	Positive	qRS (deep narrow S)	Positive
	Lateral	Basal	qRS (wide slurred S)	Flattened	qRs, Rs (wide slurred S)	Positive

		Medium	qRS (wide slurred S)	Positive	qRs, Rs (wide slurred S)	Positive
		Apical	qRS	Positive	qRS (deep narrow S)	Positive
	Posterior	Basal	QRs		Qr ,Qrs	Positive
		Medium	QRS		QrS	Positive
		Apical	QRS		qRS	Positive
	Septum	Basal	-	-	QrS	Positive
		Medium	-	-	Qs ,QrS	Positive
		Apical	-	-	QrS	Positive

RBBB, right-bundle-branch block; RV, right ventricle; LV, left ventricle; RVOT, right ventricular outflow tract.

Figure S1. Geometry of the solution domain. Supplemental data showing the mathematical algorithm for solving of the inverse problem of electrocardiography. Please see full text for details.

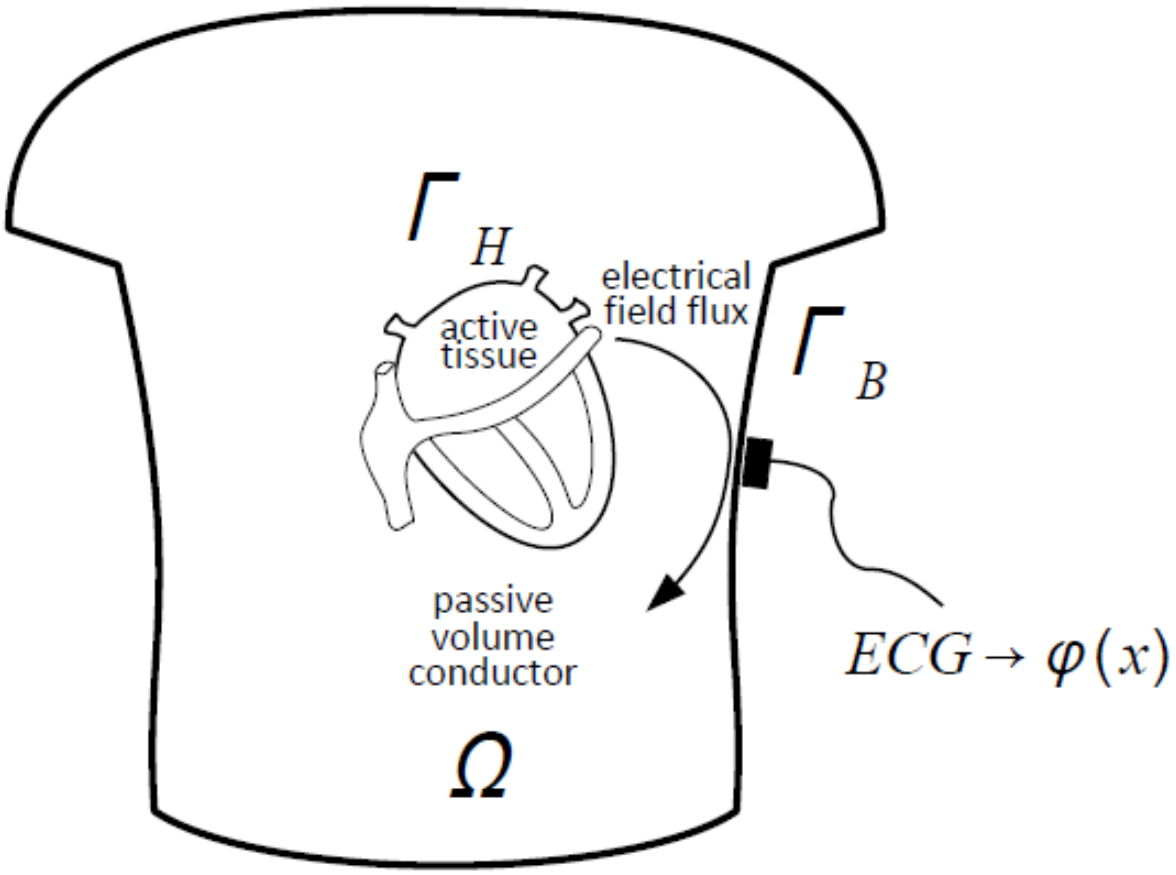

Figure S2. The results of the models merging and examples of juxtaposition of directly recorded and noninvasively reconstructed unipolar EGs. NEEES, noninvasive epicardial and endocardial electrophysiology system. 3D heart models generated by NEEES and CARTO system were merged utilizing customized software. Electroanatomical CARTO mapping data was exported and processed along with data from the noninvasively reconstructed local unipolar EGs.

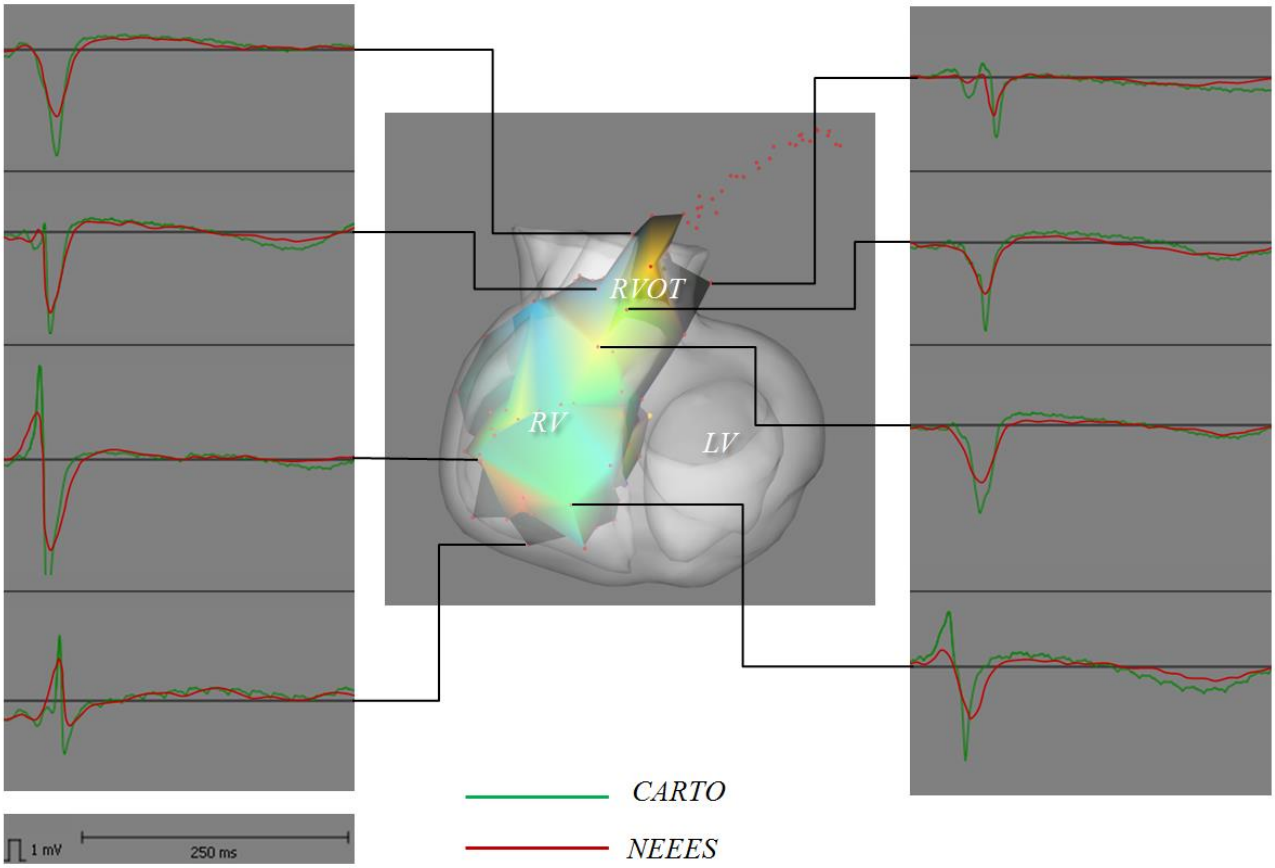

Figure S3. Example of local unipolar EGs in the RVOT in BrS patient with type-1 ECG. A. ECG in V1-V3 standard leads; coved-type ST segment elevation and negative T-wave are in V1 lead. B. Noninvasively reconstructed EGs in the epicardial aspect of the RVOT; QRS fractionation, ST-segment elevation and T-wave inversion are presented. C. Noninvasively reconstructed EGs in the endocardial aspect of the RVOT; coved-type ST segment elevation is presented.

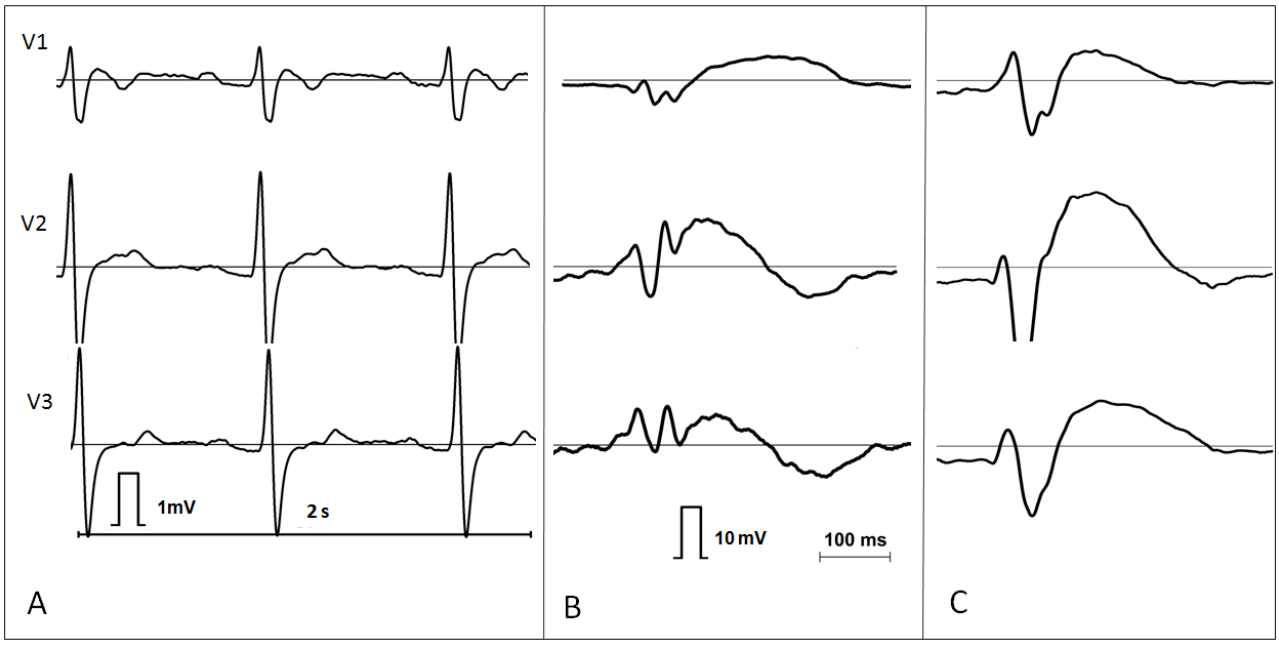

Figure S4. Local unipolar EGs, zones of elevated and fractionated EGs and ECG (I, II, III, V1, V2, V3) in the BrS patient before and after ajmaline challenge. Dotted line marked the region with abnormal EGs. Recordings of local unipolar electrograms of a BrS patient with a type-2 ECG are presented. Upper panel: before ajmaline challenge; bottom panel: after ajmaline challenge. Epicardial model on the left and endocardial model on the right, where calculations were derived from different sites of the left and right ventricle (see text for detailed description).

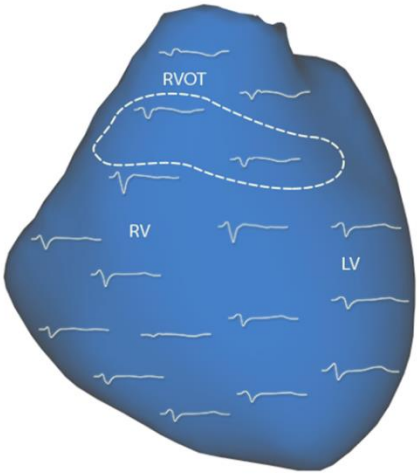
RVOT
RV
LV

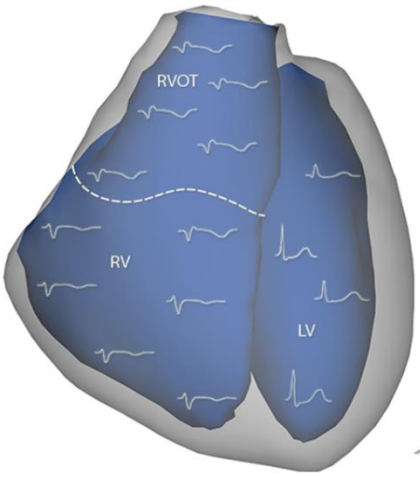
RVOT
RV
LV


I
II
III
V1
V2
V3
10 mm/mV
2 s
50 mm/s

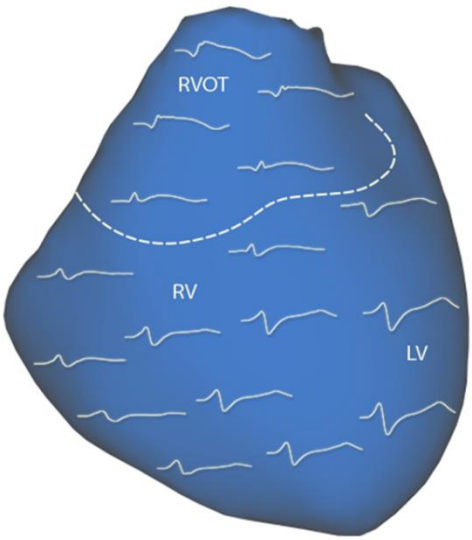
RVOT
RV
LV

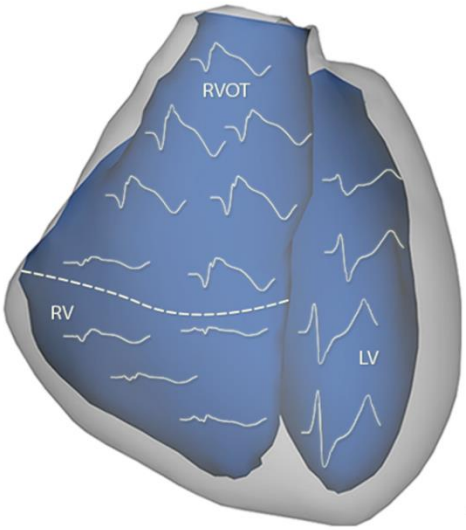
RVOT
RV
LV


I
II
III
V1
V2
V3
10 mm/mV
2 s
50 mm/s

Figure S5. Local unipolar EGs and ECG (I, II, III, V1, V2, V3) in the patient with RBBB. Recordings of local unipolar electrograms of a patient with complete right-bundle-branch-block are presented (anterior and posterior view). Epicardial model on the left and endocardial model on the right, where calculations were derived from different sites of the left and right ventricle.

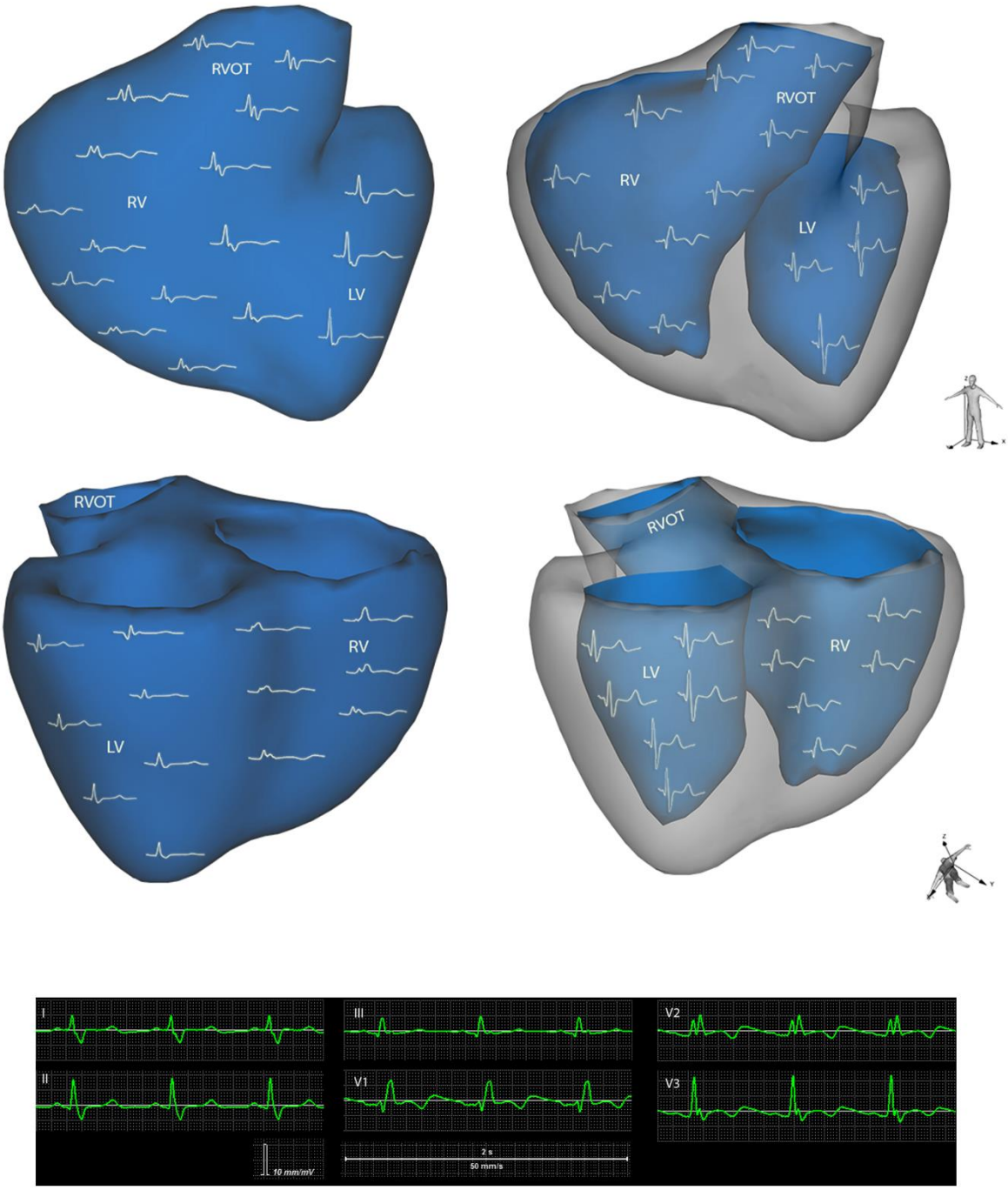

Video Legend

Video S1. LAO projection of the reconstructed 3D heart model in a patient with a spontaneous type-1 Brugada ECG is shown. Different voltage gradients between the epicardium and endocardium are color-coded from +11.4 mV (red) to -11.4 mV (purple) and shown in slow motion, based on one heart beat (depolarization and repolarization). During the terminal portion of the QRS a prominent negative voltage gradient between the epicardium and endocardium can be observed (-5.8 to -9.7 mV), predominantly located in the anatomic area of the RVOT. LAO, left anterior oblique; RBBB, right-bundle-branch-block; RVOT, right ventricular outflow tract.

Video S2. LAO projection of the reconstructed 3D heart model in a control, without overt ECG abnormalities is shown. Different voltage gradients between the epicardium and endocardium are color-coded from +28.3 mV (red) to -28.3 mV (purple) and shown in slow motion, based on one heart beat (depolarization and repolarization). During the terminal portion of the QRS a weak positive voltage gradient (0.02 to 0.8 mV) can be observed in all parts of the right ventricle, including the area of RVOT. LAO, left anterior oblique; RBBB, right-bundle-branch-block; RVOT, right ventricular outflow tract.

Video S3. LAO projection of the reconstructed 3D heart model in a patient with a typical RBBB is shown. Different voltage gradients between the epicardium and endocardium are color-coded from +12 mV (red) to -12 mV (purple) and shown in slow motion, based on one heart beat (depolarization and repolarization). During the terminal portion of the QRS a positive voltage gradient (-1.9 to -3.8 mV) can be observed in all parts of the right ventricle, not exclusively located to the area of RVOT. LAO, left anterior oblique; RBBB, right-bundle-branch-block; RVOT, right ventricular outflow tract.